Journal of Catalysis 373 (2019) 201–208

Contents lists available at ScienceDirect

Journal of Catalysis

journal homepage: www.elsevier.com/locate/jcat

Combined spatially resolved *operando* spectroscopy: New insights into kinetic oscillations of CO oxidation on Pd/γ-Al_2O_3

Ellie K. Dann [a,b], Emma K. Gibson [b,c], C. Richard A. Catlow [a,b,d], Veronica Celorrio [a,b], Paul Collier [e], Tugce Eralp [e], Monica Amboage [f], Christopher Hardacre [b,g], Cristina Stere [b,g], Anna Kroner [f], Agnes Raj [e], Scott Rogers [a,b], Alexandre Goguet [b,h,*], Peter P. Wells [b,f,i,*]

[a] Department of Chemistry, University College London, 20 Gordon Street, London WC1H 0AJ, United Kingdom
[b] UK Catalysis Hub, Research Complex at Harwell, Rutherford Appleton Laboratory, Harwell Oxon, Didcot OX11 0FA, United Kingdom
[c] School of Chemistry, Joseph Black Building, University of Glasgow, Glasgow G12 8QQ, United Kingdom
[d] Cardiff Catalysis Institute, School of Chemistry, Cardiff University, Main Building, Park Place, Cardiff CF10 3AT, United Kingdom
[e] Johnson Matthey Technology Centre, Blounts Court Road, Sonning Common, Reading RG4 9NH, United Kingdom
[f] Diamond Light Source Ltd., Harwell Science and Innovation Campus, Chilton, Didcot OX11 0DE, United Kingdom
[g] School of Chemistry, The University of Manchester, Oxford Road, Manchester M13 9PL, United Kingdom
[h] Queen's University Belfast, School of Chemistry, David Keir Building, Stranmillis Rd, Belfast BT9 5AG, United Kingdom
[i] University of Southampton, School of Chemistry, University Road, Southampton SO17 1BJ, United Kingdom

ARTICLE INFO

Article history:
Received 7 February 2019
Revised 21 March 2019
Accepted 23 March 2019

Keywords:
XAFS
DRIFTS
CO oxidation
Pd/Al_2O_3
Operando spectroscopy

ABSTRACT

Spatially resolved, combined energy dispersive EXAFS (EDE) and diffuse reflectance infrared Fourier transform spectroscopy (DRIFTS) measurements have been performed over a fixed catalyst bed of Pd/γ-Al_2O_3 during kinetic oscillations of CO oxidation. The kinetic oscillations of CO oxidation over Pd (or for that matter Pt or Rh) catalysts are a complicated phenomenon that require characterisation techniques with high time resolution and spatial resolution in order to make links between catalyst structure and surface reactivity. By measuring the extent of Pd oxidation at the nanoparticle surface, from Pd K-edge EDE, and matching this with the CO coverage, from DRIFTS spectra, at multiple positions of the fixed bed reactor it is found that the majority of the catalyst undergoes a sharp transition from the CO poisoned catalyst to the highly active, oxidised Pd surface. This transition occurs initially at the end of the catalyst bed, nearest the outlet, and propagates upstream with increasing temperature of the reactor. The oscillations in Pd surface oxide formation and CO coverage are observed only in the first ~1 mm of the bed, which gives rise to oscillations in CO_2 and O_2 concentrations observed by end-pipe mass spectrometry after the light-off temperature. The catalyst initially exists as less active, CO poisoned metallic Pd nanoparticles before light-off which transition to a highly active state after light-off when the Pd nanoparticle surface becomes dominated by chemisorbed oxygen. Kinetic oscillations only occur at the front of the catalyst bed where there is sufficient concentration of CO in the gas phase to compete with O_2 for adsorption sites at the catalyst surface. We demonstrate the complex nature of the evolving catalyst structure and surface reactivity during catalytic operation and the need for spatially resolved *operando* methods for understanding and optimising catalyst technologies.

1. Introduction

Advances to *operando* methods for characterisation of heterogeneous catalyst materials is essential for their development, particularly for uncovering structure-function relationships that govern catalytic performance [1,2]. One of the most widely investigated catalytic reactions, the oxidation of CO to CO_2, still has some aspects that remain unexplained. By looking at greater depth into the reaction kinetics of CO oxidation at a Pd, Pt or Rh surface, it

Abbreviations: DRIFTS, diffuse reflectance infrared Fourier transform spectroscopy; EXAFS, extended X-ray absorption fine structure; XANES, X-ray absorption near-edge structure; TEM, transmission electron microscopy; FTIR, Fourier transformed infrared; XAFS, X-ray absorption fine structure.

* Corresponding authors at: University of Southampton, School of Chemistry, University Road, Southampton SO17 1BJ, United Kingdom (P.P. Wells). Queen's University Belfast, School of Chemistry and Chemical Engineering, David Keir Building, Stranmillis Rd, Belfast BT9 5AG, United Kingdom (A. Goguet).

E-mail addresses: a.goguet@qub.ac.uk (A. Goguet), p.p.wells@soton.ac.uk (P.P. Wells).

https://doi.org/10.1016/j.jcat.2019.03.037
0021-9517/

is observed that the reaction oscillates spontaneously between periods of high- and low-activity under certain reaction conditions [3,4]. However, the ability of the system to undergo such kinetic oscillations is puzzling, and is yet to be fully understood [5–9]. Therefore, thorough characterisation of the oscillating catalyst must be performed with suitable time and length scale, to capture chemical and physical changes that cause such behaviour.

Previous time resolved experiments using low pressure electron microscopy to study single crystal metal surfaces found that oscillating CO oxidation was linked to the dynamic behaviour of adsorbed reactants at the catalyst surface [6,10,11]. However, these early imaging techniques were conducted in near vacuum conditions over single crystal metal surfaces – *i.e.* far from the real reaction conditions experienced by an industrial catalyst material. With the development of synchrotron radiation techniques and *operando* methods, it has been possible to close the 'materials and pressure gap' by using intense X-rays to study industrial catalysts under more realistic reaction conditions [12].

X-ray absorption fine structure (XAFS) spectroscopy is often used to characterise the active component of supported metal nanoparticle catalysts, and has been able to follow the reversible oxidation and reduction transitions of Pt, Pd and Rh catalysts during oscillating CO oxidation [13–15]. These findings are in agreement with the original theory proposed by Sales-Turner-Maple where the reactants, O_2 and CO, act as oxidising and reducing agents, respectively, for the oxidation and reduction of the metal surface under reaction conditions [7,16–18]. Although the development of the QEXAFS technique has allowed for XAFS data acquisition on the milli-second timescale, the energy dispersive approach (EDE) is able to achieve improved data quality of high time resolved measurements, by using a polychromatic X-ray beam to capture each spectrum in a 'single shot' [14,15,19,20]. Consequently, EDE methods provide a suitable tool for structural extended X-ray absorption fine structure (EXAFS) analysis of supported metal nanoparticle catalysts during oscillatory reaction kinetics [21,22].

In order to obtain conclusive evidence for the influence of the nanoparticle structure on its catalytic reactivity, the combination of *operando* EDE and diffuse reflectance infrared Fourier transform spectroscopy (DRIFTS) with on-line mass spectrometry, can be used [13,19,23–26]. The information obtained by using a combination of EDE, DRIFTS and MS has verified observations from other studies that link kinetic oscillations of CO oxidation over a Pt (or Pd, Rh) catalyst to the switching between two structural phases of the metal nanoparticle surface [14,19,24,25,27,28]. The first phase that occurs during the 'low-activity' regime is a reduced metal nanoparticle structure with high surface coverage of adsorbed CO that prevents the adsorption of O_2. The second phase that occurs during the 'high-activity' regime is an oxidised catalyst surface with high O_{ads} coverage and low CO_{ads} coverage that are able to combine at the catalyst surface in a Langmuir-Hinshelwood mechanism. However, a contradictory study by Newton *et al.* reports no evidence for the oxidation/reduction cycles of Rh during oscillating CO oxidation [14]. Instead the drive for spontaneous kinetic oscillations was suggested to result from the build-up of atomic carbon on the Rh surface, which was thought to be responsible for periodic deactivation of the catalyst and cause fluctuations in temperature upon its combustion [8,9,14]. It is clear from all of these investigations that the spontaneous kinetic oscillations over such catalytic systems is a complicated matter that requires further investigation.

For a system as complex and dynamic as the kinetic oscillations of CO oxidation, it is imperative that the combination of spectroscopic techniques is applied simultaneously to capture structure-function relationships of the catalyst [15,29,30]. Moreover, for a catalyst operating in realistic industrial applications, the spatial variation within the reactor must be considered. It has been demonstrated by recent studies using spatially resolved techniques – spatially resolved EDE [31], IR thermography [32] and SPACI-FB [33] – that the concentration gradients and temperature gradient along the axial length of a plug-flow reactor have major implications for the supported Pd, Pt or Rh nanoparticle catalyst structure and hence its reactivity [34,35]. Therefore, the combined spectroscopic techniques must have similar spatial resolution for obtaining spectral information of the same region of the catalyst bed, and probe multiple positions along the length of the reactor for complete spatial analysis.

Performing the simultaneous EDE and DRIFTS measurements with time and spatial resolution is far from trivial. A suitable reaction chamber must be used that allows the catalytic reaction to proceed whilst positioned in the appropriate geometry for transmission of X-rays through the sample and reflection of IR from its surface [36]. Moreover, the design of the reaction chamber must allow for transmission of both spectral beams to probe the sample at multiple axial positions of the catalyst bed. In this work, an oscillating CO oxidation reaction over a Pd/Al_2O_3 catalyst is investigated, with simultaneous EDE and DRIFTS performed at multiple spatial positions along the length of a fixed catalyst bed, and catalytic activity measured by end-pipe mass spectrometry. This initial study has focussed on Pd/Al_2O_3 as it is a system where kinetic oscillations of CO oxidation is known to occur. Using this new approach, the electronic properties, local atomic structure and surface reactivity of the Pd nanoparticles were followed in real time to probe the behaviour of the catalyst at different positions within the reactor. This approach has allowed for thorough characterisation of a fixed catalyst bed of supported Pd nanoparticles during CO oxidation, providing new insights for the evolution of the reaction profile of an entire catalyst bed operating in plug-flow configuration during kinetic oscillations.

2. Experimental section

2.1. Sample preparation

A 3 wt% $Pd/\gamma\text{-}Al_2O_3$ catalyst, with average Pd particle diameter 1.1 nm, was prepared by incipient wetness impregnation of an aqueous solution of tetraamminepalladium(II) hydroxide (5.96 wt% Pd, Johnson Matthey) onto a $\gamma\text{-}Al_2O_3$ support (SASOL), followed by calcination (500 °C, 2 h). The detailed characterisation of this catalyst sample, including particle size analysis, is reported elsewhere [30].

2.2. EDE/DRIFTS measurements

Experiments were carried out on I20-EDE, the energy dispersive beamline of Diamond light source, Didcot, UK. Dispersive XAFS at the Pd K-edge (24358 eV) were collected in transmission mode using a Si(3 1 1) polychromator and a FReLoN CCD camera as the X-ray detector [37]. The dispersive X-ray beam was focussed at the sample to a spot size of 0.5 mm horizontally and 0.15 mm vertically. The beam intensity was reduced by a factor of 5 by opening the wiggler gap to negate radiation damage to the sample. To check that the X-rays were not causing photoreduction of the sample, EDE spectra were collected continuously at multiple positions under the reactant gas feed (Supporting information, Fig. S2). The reaction cell used for synchronous, spatially resolved EDE and DRIFTS measurements was designed at the UK Catalysis Hub. The reaction cell (Fig. 1) was constructed from pure grade aluminium with a square cross sectional channel, measuring 5 mm × 5 mm, to contain the catalyst sample. The aluminium walls on two sides of the reactor were thinned to 250 μm by drilling a 50 mm length

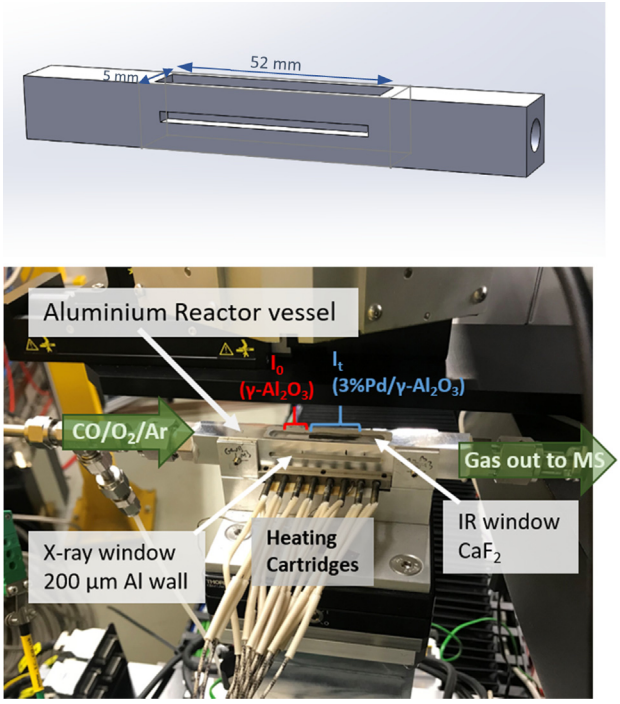

Fig. 1. (a) Schematic drawing of the new EDE/DRIFTS reaction cell design. (b) Photograph of the aluminium EDE/DRIFTS reaction cell mounted on I20-EDE beamline, Diamond Light Source. The reactor is loaded with bare γ-Al_2O_3 and Pd/γ-Al_2O_3 catalyst and connected to gas lines at either end.

trench along the sample channel for transmission of X-rays through the cell and sample. A rectangular 52 mm × 7 mm CaF_2 window was fitted to the top face of the reactor for IR transmission to and from the catalyst surface. Gas lines were fitted to both ends of the cell with Swagelok fittings and a K-type Inconel thermocouple was inserted through one end of the reactor to measure the temperature of the catalyst sample. The tip of the thermocouple was positioned at the end of the reactor nearest the reactor outlet and so measured the local temperature at the end position of the catalyst bed. A heating plate was positioned beneath the reactor, and controlled by an external thermocouple. An Agilent Carey 680 FTIR Spectrometer was positioned in the experimental hutch and used a DaVinci arm accessory fitted with praying mantis optics to refocus the IR beam to the catalyst surface within the EDE/DRIFTS cell. Mass spectrometry data of the reactor exhaust was collected using a Hiden QGA for online end-pipe analysis.

400 mg of the Pd/γ-Al_2O_3 catalyst and 200 mg of bare γ-Al_2O_3 were sieved to a pellet fraction of 250–355 µm and loaded separately into the reactor so that the γ-Al_2O_3 sat upstream of the catalyst, and was held in place by quartz wool. The bare γ-Al_2O_3 was used as a reference to account for the absorption and scattering of the polychromatic X-ray beam by the support material, and as the background for DRIFTS spectra. The Pd/γ-Al_2O_3 catalyst bed extended a length of 18 mm and EDE/DRIFTS measurements were collected at 8 different spatial positions along its length; 0.4, 1.8, 5.2, 7.1, 8.7, 10.4, 12.5 and 14.6 mm from the front of the bed. The catalyst was pre-treated with 4%H_2/Ar at 135 °C then cooled to room temperature in Ar to reduce and clean the catalyst prior to each run. The reactant gas feed (1%CO/3%O_2/Ar) was introduced to the sample at a total flow rate of 50 ml min^{-1} and allowed to reach steady state before ramping the temperature 2 °C min^{-1} to 135 °C collecting EDE, DRIFTS and MS measurements continuously. Each EDE spectrum was acquired in 4.8 ms to collect information of the XANES region and used 200 accumulations for EXAFS analysis. DRIFTS spectra were collected with 64 accumulations per spectrum, giving a time resolution of 25 s per spectrum and using a background collected from the bare γ-Al_2O_3 surface, in the reactant (CO/O_2/Ar) gas feed. The reaction times and activity for each run were synchronised in the spatio-temporal analysis by matching the light-off of CO (large spike in CO_2 formation) from the end-pipe mass spectrometry, which was consistent for each run. The MS signal was normalised relative to the Ar signal (m/z = 40) to account for any detector variation. The CO signal (m/z = 28) was corrected for contributions from CO_2 fragmentation by subtracting 10% of the value of m/z = 44.

2.3. EXAFS analysis

Processing the time resolved EDE data was made using the DAWN software package in order to crop, calibrate and normalise the XAFS spectra.[18] The processing of the Extended X-ray Absorption Fine Structure (EXAFS) data was performed using IFEFFIT with the Horae package (Athena and Artemis). Athena was used to calibrate, align and normalise the spectra with respect to the Pd foil, for which E_0 was set at 24358 eV. EXAFS data processing of k^2 data used an appropriate k range for the data (3.2 to 13.4 $Å^{-1}$). The k-weighting of 2 was chosen for balanced scattering contribution from atomic neighbours with low Z values (O) and high Z values (Pd) [38]. Analysis of the Fourier transformed data was limited to fitting the first Pd-Pd (2.734 Å) scattering path of Pd foil, and Pd-O (2.018 Å) and Pd-Pd (3.030 Å) scattering paths of bulk PdO. The amplitude reduction factor, S_0^2, was derived from fitting the Pd K-edge EXAFS of Pd foil using a fixed Pd-Pd coordination number of 12 to give a value of 0.81, shown in supporting information Fig. S3. Linear combination fitting was performed for XANES spectra ($-20 < E_0/\text{eV} < 50$), using two reference spectra for $Pd^{(0)}$ and $Pd^{(II)}$. The fitting model used a linear combination of $Pd^{(0)}$ and $Pd^{(II)}$, such that the sum was forced to equate to 1. The reference spectrum for $Pd^{(0)}$ was collected of the Pd/γ-Al_2O_3 catalyst in a reducing atmosphere of 4% H_2/Ar at 100 °C. The reference spectrum for $Pd^{(II)}$ was collected of the initial calcined catalyst PdO/γ-Al_2O_3 at room temperature.

2.4. IR thermography imaging

Optris PI 160 thermal imaging camera was used to capture 2D images of the IR emission from the reactor containing the same Pd/γ-Al_2O_3 catalyst during the CO oxidation temperature ramp experiment (gas feed 1%CO/3%O_2/Ar; flow rate 50 ml min^{-1}; temperature ramp 2 °C min^{-1}).

3. Results and discussion

3.1. End-pipe catalytic activity

The concentration of reactant and product gases (CO, O_2 and CO_2) from the reactor exhaust during the temperature ramp experiment are shown in Fig. 2. The reaction profile shows an exponential increase in CO consumption and formation of CO_2 with increasing temperature until a critical temperature (114 °C), at a reaction time of 500 s, when CO conversion increased suddenly to 100%. This critical temperature will be referred to herein as the light-off point. At the light-off point, a large increase in CO_2 formation is observed which led to CO_2 production and O_2 consumption exceeding the values expected from the amount of CO consumed, considering the stoichiometry of the reaction. The sample temperature reported in Fig. 2 shows a small deviation from the linear temperature ramp at a reaction time of 500 s due to heat released from exothermic CO oxidation at the light-off point. As the temperature was increased beyond this light-off point, the CO conversion remained at 100% but the O_2 consumption and CO_2

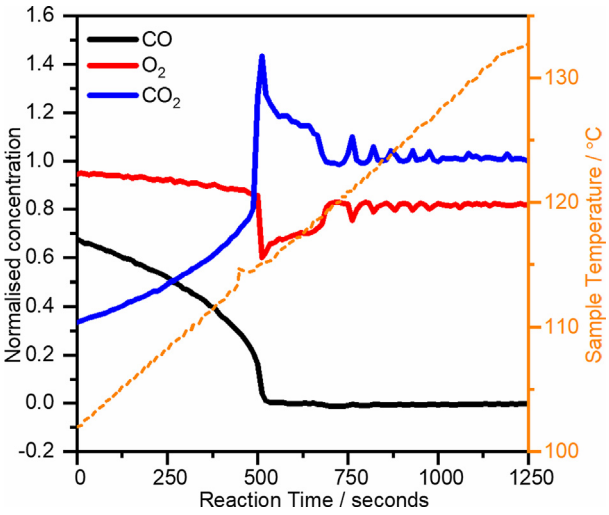

Fig. 2. Mass spectrometry analysis of exhaust gas from plug-flow reactor during CO oxidation temperature ramp experiment with 1%CO/3%O_2/Ar over the Pd/γ-Al_2O_3 catalyst, showing CO concentration (black), O_2 concentration (red) and CO_2 concentration (blue) calculated relative to inlet CO signal from mass spectrometry and measured internal catalyst temperature (orange, dashed).

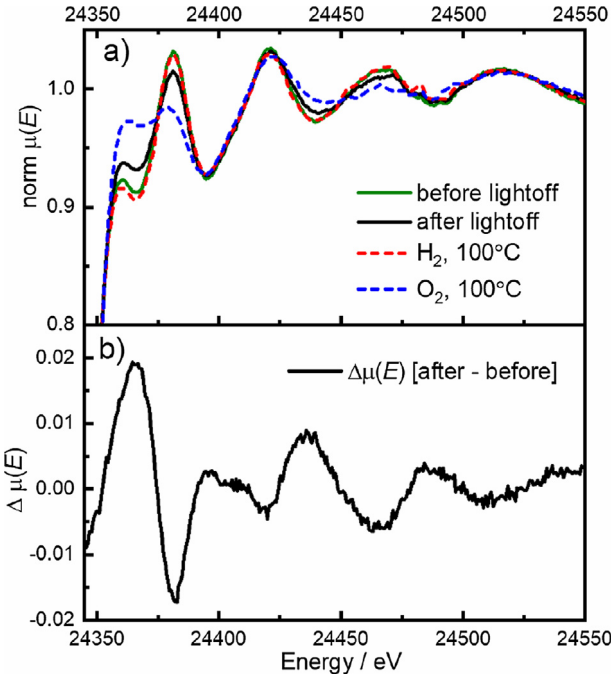

Fig. 3. (**a**) Pd K-edge XANES spectra of Pd/γ-Al_2O_3 catalyst at position 8 (14.6 mm) in a plug-flow reactor under reactant (1% CO/3% O_2/Ar) gas feed, before (green) and after (black) ignition for CO oxidation. Plotted together with *ex situ* measurements of Pd/γ-Al_2O_3 catalyst after reduction treatment in 4% H_2 at 100 °C (red) and then exposure to 10% O_2 at 100 °C (blue) and (**b**) difference spectrum of Pd K-edge XANES before and after ignition for CO oxidation.

formation started to oscillate with a time period of about 50 s. As the temperature was increased further, the amplitude of the oscillations decreased until the CO_2 formation and O_2 consumption plateaued at reaction time 1000 s (reactor temperature 127 °C), with normalised concentration of 1 and ~0.8 for CO_2 and O_2, respectively. The same reaction profile, as shown in Fig. 2, was reproduced from the catalyst with each run, showing that the catalyst was regenerated to its original state after each cleaning/reduction cycle (Supporting Information, Fig. S4).

3.2. Combined EDE/DRIFTS

3.2.1. Position 8 – end of catalyst bed (14.6 mm)

The Pd K-edge XANES spectra of the Pd/γ-Al_2O_3 catalyst in the reactant (CO/O_2/Ar) gas feed were collected throughout the temperature ramp (80–135 °C) at eight different spatial positions along the length of the 18 mm catalyst bed. The data collected from the end of the bed, nearest to the reactor outlet (position 14.6 mm from the front of the catalyst bed) is discussed first. The XANES spectra collected before and after light-off at 114 °C are shown in Fig. 3(a), together with their difference spectrum (Fig. 3(b)). XANES spectra of the catalyst collected under a reducing (4% H_2, 100 °C) and oxygen (10% O_2, 100 °C) environment are also shown for reference. The XANES spectrum of Pd/γ-Al_2O_3 catalyst under reaction conditions before light-off matches that of the reference spectrum collected under the reducing (H_2) environment. By fitting the corresponding Fourier transformed EXAFS data (plotted in supporting information, Fig. S7) to a model using a single Pd-Pd scattering path of Pd foil, the Pd/γ-Al_2O_3 catalyst before light-off is shown to have a Pd-Pd bond distance consistent with fcc Pd metal structure (2.733 Å) and a coordination number, 7.8 (detailed in Table S1). This fitting model corresponds to metallic Pd nanoparticles with an average diameter of 2.7 nm (calculated by a method reported previously [39], detailed in supporting information, Table S2).

After light-off, an increase in intensity of the main edge transition at 24370 eV is observed, due to increased vacant electronic states of Pd species in a higher oxidation state. This difference in Pd K-edge XANES features with respect to the pre light-off measurement is even clearer from the difference spectrum plotted in Fig. 3(b). The XANES spectrum after light-off could not be matched entirely to that of the reference spectra collected under oxidising or reducing environment, which highlighted that only partial oxidation had occurred. By fitting the corresponding Fourier transformed EXAFS data (shown in supporting information Fig. S8) to a suitable model using scattering paths of Pd-O (2.00 Å) for bulk PdO and Pd-Pd (2.725 Å) for Pd foil, the catalyst could be described as metallic Pd nanoparticles, with average Pd-Pd coordination number of 6.5, and average Pd-O coordination number of 0.8. The absence of a Pd-Pd scattering path at ~3.0 Å for bulk PdO structure meant that the Pd oxidation was limited to the nanoparticle surface. The oxidation is likely to be limited only to Pd at the nanoparticle surface because these reaction conditions (114 °C) are below the temperature at which the complete bulk PdO formation is expected to occur (>200 °C) [40]. This result is consistent with previous EXAFS analysis of bulk Pd metal nanoparticles with average particle diameter of ~2 nm and a surface oxide layer [41]. The reference spectrum collected under oxygen (O_2/Ar, 100 °C) atmosphere displayed similar scattering features, but with a greater contribution from Pd-O scattering due to greater surface oxygen coverage, showing that under the reaction conditions for CO oxidation the surface is not saturated with oxygen.

The DRIFTS spectrum of the Pd/γ-Al_2O_3 catalyst under reaction conditions before light-off (114 °C) is reported in Fig. 4. The spectrum shows characteristic absorption bands for CO adsorbed on a metallic Pd surface (CO_{ads}) by linear (2064 cm^{-1}), bridged (1972 cm^{-1}, 1928 cm^{-1}) and multi- coordination [42–46]. These bands were present on the catalyst at 113.9 °C before light-off, then decreased in intensity at 114.7 °C, and were lost completely by 115.4 °C showing that the concentration of CO species remaining adsorbed to the catalyst surface after light-off was below the detection limit. The absorption bands at 1580 cm^{-1} and 1458 cm^{-1} can be attributed to carbonate species at the catalyst surface which were not removed at the light-off temperature [47,48]. These carbonates may be strongly adsorbed to the γ-Al_2O_3 surface and, most likely, do not participate in catalysis at the Pd nanoparticle surface [48].

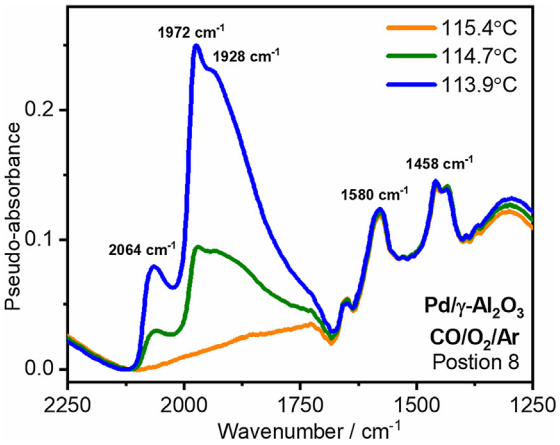

Fig. 4. *Operando* DRIFTS spectra of Pd/γ-Al_2O_3 catalyst in plug-flow reactor at position 8 (nearest the end of the catalyst bed) during reactant (1% CO/3% O_2/Ar) gas flow at increasing temperatures.

Interestingly, the carbonyl bands, while they decreased in intensity during light-off, did not change stretching frequency, meaning that CO adsorption was only observed on metal Pd sites. There was no evidence for the adsorption of CO on $Pd^{(II)}$ sites, nor evidence of dipole coupling that has previously been reported to shift the CO stretching frequency as a function of CO_{ads} coverage [49].

Further analysis of the XANES data involved linear combination analysis of XANES spectra at increasing time points across the light-off period (supporting information, Fig. S9). The $Pd^{(II)}$ component increased from 0.05 to 0.2, and the $Pd^{(0)}$ component decreased from 0.95 to 0.8, due to partial Pd oxidation at the nanoparticle surface as inferred from EXAFS analysis. The extent of Pd oxidation can be followed directly from the XANES spectra by plotting the absorption intensity of the main edge transition of at 24370 eV (referred to as the whiteline intensity herein). The increase in the whiteline intensity with reaction time is plotted in Fig. 5, together with the intensity of the CO stretching band at 1940 cm^{-1} of the DRIFTS spectra recorded at the corresponding spatial position.

The results reported in Fig. 5 suggest that the oxidation of Pd at the nanoparticle surface coincided with the loss of CO_{ads} from the surface at the light-off temperature (114 °C) and a reaction time of 440 s. This observation is consistent with the widely accepted model which assumes that, beyond the light-off temperature, the surface is dominated by atomic oxygen and the reaction kinetics for combination of CO_{ads} with surface oxygen are so fast that the carbonyl surface concentration is too low to be detected by DRIFTS spectroscopy [50]. The large amount of CO_2 detected by MS at this reaction time (500 s) and high CO conversion indicates fast reaction kinetics which supports the latter assumption.

3.2.2. Position 1 – front of catalyst bed (0.4 mm)

The Pd K-edge XANES of the Pd/γ-Al_2O_3 catalyst measured at a position 0.4 mm from the front of the catalyst bed showed that the palladium was fully reduced before light-off and formed a surface oxide after light-off (Fig. S10), similarly to the catalyst at the end of the reactor. However the onset of oxide formation occurred at a much later reaction time (620 s) and therefore higher light-off temperature (117.5 °C). Moreover, this transformation was accompanied with oscillating behaviour rather than a sharp, direct transition. By plotting the whiteline intensity together with the intensity of the CO stretching band at 1940 cm^{-1} of the DRIFTS spectra (Fig. 6), it was possible to observe clearly that these oscillations occurred both in the Pd surface oxide formation and the CO surface coverage.

The oscillations in Pd oxide formation and CO surface coverage were also found to coincide with the oscillations observed in O_2 consumption and CO_2 formation measured with the end-pipe mass spectrometry signal (from a reaction time of 650 s to 1000 s in Fig. 6). During these oscillations, the sequential behaviour was observed: a rise in CO_2 formation coinciding with a drop in CO coverage due to conversion of previously adsorbed CO into CO_2, which was followed by a sharp increase in the extent of Pd oxidation, then a period of lower CO_2 conversion coinciding with an increase in

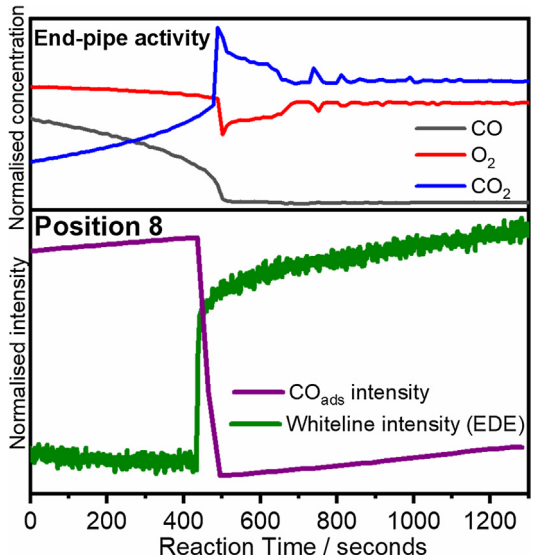

Fig. 5. Bottom panel shows EDE Pd K-edge white line intensity (green) and DRIFTS CO adsorption intensity (purple) of catalyst Pd/Al_2O_3 at spatial position 8 (nearest to the reactor outlet) of the fixed catalyst bed in reactant (1% CO/3% O_2/Ar) gas feed during temperature ramp experiment (100–135 °C). Top panel shows the simultaneous end-pipe mass spectrometry signals for O_2 (red), CO (black) and CO_2 (blue) concentrations of the reactor exhaust.

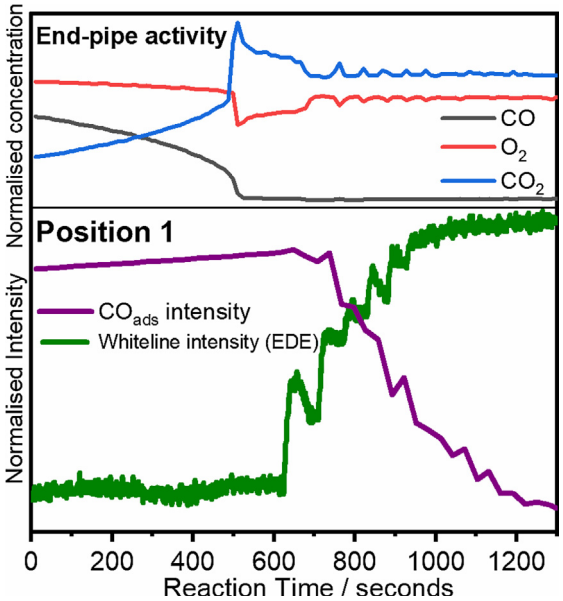

Fig. 6. Bottom panel shows EDE Pd K-edge white line intensity (green) and DRIFTS CO adsorption intensity (purple) of catalyst Pd/Al_2O_3 at spatial position 1 (nearest to the reactor inlet) of the fixed catalyst bed in reactant (1% CO/3% O_2/Ar) gas feed during temperature ramp experiment (100–135 °C). Top panel shows the simultaneous end-pipe mass spectrometry signals for O_2 (red), CO (black) and CO_2 (blue) concentrations of the reactor exhaust.

surface carbonyl concentration. With each cycle, the whiteline intensity increased to a greater value (*i.e.* Pd became more oxidised) and the CO coverage decreased to a lower value until the catalyst eventually reached the same state of apparent zero CO coverage and partial Pd oxidation similar to that at the position at the end of the catalyst bed. Consequently, the overall behaviour in terms of temperature dependence of the CO conversion, Pd oxidation state and carbonyl coverage is similar to that observed at the position near the reactor outlet with the notable exception of an oscillatory component convolution. The changes to the gas concentrations observed during the reaction period before 650 s were not reflected in the EDE or DRIFTS data of Fig. 6 because the catalytic activity at earlier reaction times (and lower temperatures) was governed by the portion of catalyst bed downstream of position 1, as discussed later.

3.2.3. Spatio-temporal analysis

In order to further the analysis of the catalyst structure and reactivity across the entire catalyst bed, the time resolved XAFS and DRIFTS spectra were compared at 8 different spatial positions along the length of the catalyst bed. The extent of oxidation (shown by the whiteline intensity) and the CO coverage (shown by intensity of DRIFTS absorption band at 1940 cm^{-1}) are plotted in Fig. 7 for all 8 spatial positions as a function of reaction time. The top panel refers to the position measured nearest to the reactor inlet (position 1), and positions measured at increasing distance from the reactor inlet are plotted in order vertically down the figure with the position nearest to the reactor outlet (position 8) shown in the bottom panel. The sharp increase in whiteline intensity is observed for all spatial positions downstream of position 2, with oscillations in Pd oxidation observed most prominently at position 1, and to a lesser extent at position 2. The sharp increase in whiteline intensity occured at the earliest reaction time (440 s, 114 °C) at position 8 – nearest to the reactor outlet – secondly at positions 7 and 6 (460 s, 115 °C) and subsequently at positions 5 to 3 (500–530 s) – in the middle of the catalyst bed. The CO coverage is found to decrease in intensity at the same time as the Pd oxidation at each position, which can be explained by the ignition of adsorbed CO to CO_2 upon oxidation of the Pd surface. The fast reaction kinetics of CO oxidation over a Pd oxide surface are assumed to continue to operate via a Langmuir-Hinshelwood mechanism; however the rapid combination of CO_{ads} and O_{ads} means that CO_{ads} are short lived and are not present on the oxide surface at concentrations enough to be observed by DRIFTS measurements. The increase in whiteline intensity at position 2 (1.8 mm from the front of the catalyst bed) occurs at a later reaction time than at positions 3 – 8. The whiteline intensity increases, then shows a slight decrease before increasing further to the partially oxidised state. The CO_{ads} intensity at position 2 also does not follow a sharp decrease but displays a gradual one with some oscillating behaviour. The oscillations observed at position 2 are less pronounced than those at position 1, and can result from the changes in the CO concentration and temperature due to larger oscillations of reaction kinetics upstream.

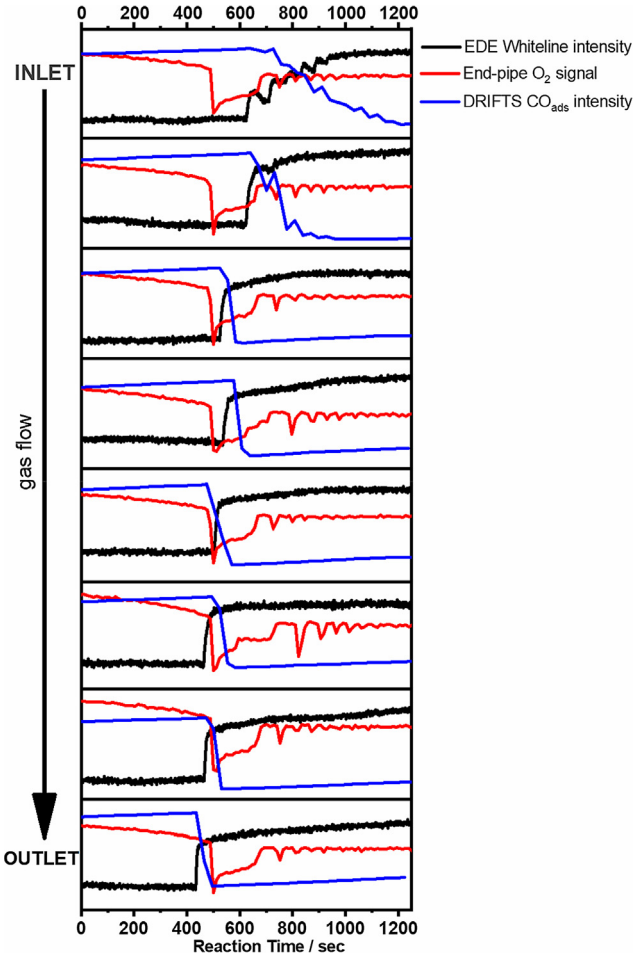

Fig. 7. End-pipe mass spectrometry O_2 concentration (red), DRIFTS CO adsorption intensity (blue) and EDE Pd K-edge white line intensity (black) at multiple spatial positions (achieved through a series of consecutive temperature ramp experiments) in the Pd/γ-Al_2O_3 fixed catalyst bed from the front/inlet (top panel) to the end/outlet (bottom panel) during each temperature ramp experiment (100–135 °C) during flow of reactant gas feed (1% CO/3% O_2/Ar).

The integral activity of the complete catalyst bed as shown by the end-pipe mass spectrometry signal (Fig. 2) can be explained by considering the Pd oxidation and CO coverage at each of the 8 investigated spatial positions. The reaction front is initiated at the end of the catalyst bed nearest to the outlet at reaction time 440 s, and propagates upstream until the majority of the catalyst bed (positions 3 – 8) have consumed oxygen for the formation of the Pd oxide surface and the ignition of the adsorbed CO by a reaction time of 590 s (reactor temperature 118 °C). The large consumption of O_2 observed during this reaction period (440–590 s) is matched by the large formation of CO_2 due to ignition of 'stored' CO adsorbed on the metal surface causing the apparent conversion to reach a value greater than 1 with respect to the inlet CO conversion. After this period, the CO_2 formation and O_2 consumption fall to the value expected from stoichiometry which is governed by the high conversion rate of CO oxidation over the oxidised catalyst downstream of position 2. The oscillations in O_2 consumption and CO_2 formation are observed by end-pipe analysis between 700 and 1000 s (reactor temperature 120–128 °C), which coincides with the reaction time at which oscillations in CO coverage and Pd oxidation were observed in the first 0.4 mm of the catalyst bed (position 1). Beyond 1000 s reaction time, the oscillations ceased and CO_2 formation was maintained at its maximum value with respect to the CO conversion.

Interestingly, oscillatory behaviour was observed for the concentrations of the reactants and products measured with the end-pipe mass spectrometer even though the majority of the catalyst bed was not displaying any oscillation with respect to its structure or population of adsorbates. Examining closer these "end-pipe" oscillations, it is possible to see that they are observed in the post light-off region of the front section of the catalyst bed. In the context of a reaction displaying a light-off behaviour, it is important to recognise that the light-off position with respect to the catalyst bed axial position will change with reaction temperature; *i.e.* the higher the temperature the closer the light-off position

to the reactor inlet. Another aspect to consider is that once the light-off position with respect to the bed is passed, the remaining fraction of catalyst present downstream of the position will be "unused". Indeed, at (or very closely after) the light-off position, the reactant is fully converted, the remaining catalyst after this point has nothing left to convert and is therefore not engaged in any catalysis. In the context of the present reaction, we can see that the oscillations observed with the mass spectrometer are visualised closely after the light-off point observed at the front of the catalyst bed (position 1). So, we can see that after the light-off point has been reached for the front end of the bed, the oscillation will propagate downstream of a remaining "idle" catalyst bed with limited interaction to alter them except potentially for physical processes such as axial dispersion. Although the majority of the catalyst bed beyond the light-off temperature is not engaged in the catalysis, the Pd species from position 3–8 are present in the oxidised state and are able to capture and convert any CO that slips through the oscillating region at the front of the bed. For this reason, the CO concentration from end-pipe mass spectrometry beyond 114 °C (500 s) always measures complete conversion, even during oscillations at the front of the bed. However, fluctuations in the CO_2 concentration formation arise when CO_2 is produced from the combustion of stored CO at the front of the bed – observed by DRIFTS at position 1 – as well as conversion of the inlet CO feed, forming an over stoichiometric amount of CO_2. Equally, under-stoichiometric amount of CO_2 are observed during low-activity period of the oscillations when CO from the inlet gas feed is used to increase the CO coverage of the metal surface, rather than direct conversion to CO_2. Similarly, fluctuations in the O_2 consumption occur when the O_2 from the inlet gas feed is used not only in the oxidation of CO from the inlet gas feed but also in the oxidation of additional stored CO and oxidation of the Pd surface itself.

The oxidation of CO is an exothermic reaction ($\Delta H = -282$ KJ mol^{-1} [51] and so the reaction front coincides with a temperature hotspot that can be observed with an infrared camera. An infrared camera positioned above the EDE/DRIFTS reactor was able to follow the position of the reaction front in the Pd/γ-Al_2O_3 catalyst bed during the CO oxidation reaction period. Fig. 8 reports the thermographic IR images of the reactor, each panel showing a snapshot at increasing reaction time from 528 secs (top panel) to 924 secs (bottom panel). The first image in the top panel of Fig. 8 shows a moderate hotspot at a position of ~18 mm along the catalyst bed upon initial light-off at 114 °C. The position of this hot spot confirms that the CO is first ignited from a position nearest to the outlet of the reactor, in line with the measurements of CO coverage and Pd oxidation from spatially resolved DRIFTS and EDE, respectively. As the reaction time proceeds, the global increase in temperature of the reactor (from the external heater) and the local increase in temperature due to exothermic reaction at the end of the catalyst bed results in the reaction rate increasing and the reaction front moving upstream since "less" catalyst is needed to achieve similar conversion performance. These observations are again in line with EDE and DRIFTS measurements which show the change in Pd oxidation and CO coverage, respectively. The reaction front is shown finally to move towards the front of the bed at a later reaction time of ~700 secs where the catalyst undergoes oscillating behaviour due to the relatively high concentration of incoming CO which competes with oxygen for adsorption sites at the catalyst surface and delays the sharp oxidation of the catalyst surface.

These results therefore confirm that the CO oxidation reaction proceeds at the Pd nanoparticle surface via the Langmuir-Hinshelwood mechanism, whereby both molecular CO and atomic oxygen must be adsorbed before reaction to form CO_2 [52]. Our data agrees with the proposition that the dissociative adsorption of oxygen is prohibited at low temperatures, due to the high surface coverage of CO, which gives rise to a 'low-activity' regime [27]. This low-activity occurs below the light-off point when dissociative adsorption of O_2 is the rate limiting step. For the light-off to occur there must be sufficient desorption of CO to allow the dissociative adsorption of O_2 and subsequent reaction at the catalyst surface to form CO_2. For the majority of the catalyst bed, there was a sharp transition at this point from the low-activity to high-activity regime as the vacant sites created after reaction to form CO_2 were filled with atomic oxygen and the surface oxide proceeded to catalyse the CO oxidation at a much faster rate, similarly to that the Pt systems investigated in the past.[8b, 9, 28] The light-off occurs initially at the end of the catalyst bed where there is the lowest CO concentration and greatest temperature, due to the propagation of CO conversion and reaction exotherms, respectively. The low CO concentration at the outlet is characteristic of the reactant gradient within a fixed bed reactor, and results in there being less competition for the dissociative adsorption of oxygen [33]. The reaction becomes self-accelerating at this point as an increasing number of vacant adsorption sites are created after the formation of each CO_2 molecule and the local temperature is raised by the exothermic reaction. The conditions for oscillating behaviour hold only within the first ~1 mm of the catalyst bed, similarly to an Rh catalyst bed in a previous study, due to the high concentration of CO at the inlet compared to all further positions downstream [31]. This point is where, after reaction to form CO_2, the vacant adsorption sites are refilled by poisoning CO rather than O_2, and thus the reaction rate is slowed to the 'low-activity' regime. Only upon desorption or ignition of surface adsorbed CO can the dissociative adsorption of O_2 occur and the light-off process to start again.

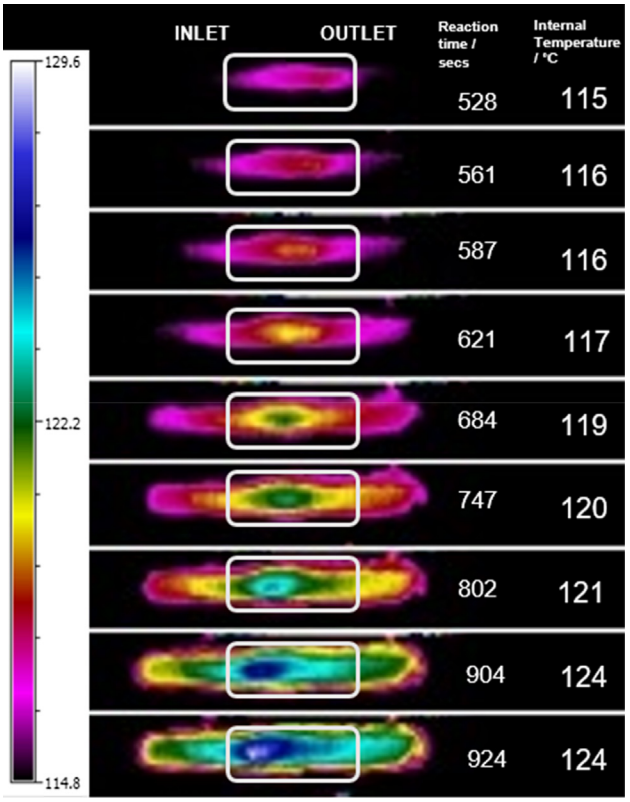

Fig. 8. Thermographic IR images of reactor during CO oxidation (1%CO/3%O_2/Ar) at increasing temperatures (115–124 °C). Gas flow from inlet (left) to the outlet (right), annotated with the temperature read from the internal thermocouple positioned in the catalyst bed. The location of the catalyst bed within the reactor is outlined by a white box.

4. Summary and conclusions

A custom-built reactor has been designed for a combined, spatially resolved XAFS and DRIFTS measurements of a catalyst operating under reaction conditions. The spatially resolved measurements of both the metal oxidation state, from Pd K-edge EDE measurements, and surface speciation, from DRIFTS measurements, have been able to provide new insights for the operation of a Pd/γ-Al_2O_3 catalyst bed. The structural and functional behaviour at different spatial positions can be combined to explain the end-pipe catalytic activity.

The ignition of CO oxidation at the Pd nanoparticle surface has been found to coincide with the oxidation of the Pd nanoparticle surface. This confirms that CO oxidation proceeds with fast reaction kinetics via a Langmuir Hinshelwood mechanism once there is the dissociative adsorption of oxygen at the Pd surface. The Fourier transformed EXAFS show that this Pd oxidation is limited only to the nanoparticle surface within the operating temperature range (<140 °C), with the bulk of the particle remaining as metallic Pd.

The oxidation of the Pd surface and ignition of stored CO_{ads} is a fast transition for the majority of the catalyst bed at the light-off temperature (114 °C). Initially, the CO ignition occurs at the end of the catalyst bed, and the reaction front propagates upstream with increasing temperature. The periodic oscillations of CO oxidation over the supported Pd nanoparticle catalyst (Pd/γ-Al_2O_3) occur only at the front of the catalyst bed, after the light-off temperature. The oscillations are observed by end-pipe analysis of CO_2 and O_2 concentrations and result from the competition between CO storage and surface oxide formation at the nanoparticle surface.

Author contributions

The manuscript was written through contributions of all authors. All authors have given approval to the final version of the manuscript.

Funding sources

UK Catalysis Hub Consortium, United Kingdom and EPSRC, United Kingdom (portfolio grants EP/K014706/1, EP/K014668/1, EP/K014854/1, EP/K014714/1 and EP/I019693/1.

Acknowledgment

The authors acknowledge Diamond Light Source beamline staff, in particular Sofia Diaz-Moreno, Luke Keenan, Darren Neville and Trevor Orpin, for provision of beamtime at I20-EDE (Experiment SP17340) for collection of the data presented in this work, and also at B18 (Experiment SP17725) for development of the experimental set-up. The RCaH are acknowledged for use of facilities and staff support. UCL and EPSRC are thanked for the iCASE studentship of E.K.D. UK Catalysis Hub is thanked for resources and support provided via our membership of the UK Catalysis Hub Consortium (portfolio grants EP//K014706/1, EP/K014668/1, EP/K014854/1, EP/K014714/1 and EP/I019693/1).

Appendix A. Supplementary material

All data supporting this study are openly available from the University of Southampton repository at https://doi.org/10.5258/SOTON/DO857. Supplementary data to this article can be found online at https://doi.org/10.1016/j.jcat.2019.03.037.

References

[1] B.M. Weckhuysen, Chem. Soc. Rev. 39 (2010) 4557.
[2] M.A. Bañares, Adv. Mater. 23 (2011) 5293.
[3] In M.S.k. Marina and I.J. Nils (Editors), Studies in Surface Science and Catalysis, Vol. Volume 86, Elsevier, p. 47; 1994.
[4] M.P. Cox, G. Ertl, R. Imbihl, Phys. Rev. Lett. 54 (1985) 1725.
[5] S. Hong, H.H. Richardson, J. Vac. Sci. Technol., A 11 (1993) 1951.
[6] J. Lauterbach, G. Haas, H.H. Rotermund, G. Ertl, Surf. Sci. 294 (1993) 116.
[7] J.E. Turner, B.C. Sales, M.B. Maple, Surf. Sci. 103 (1981) 54.
[8] V.A. Burrows, S. Sundaresan, Y.J. Chabal, S.B. Christman, Surf. Sci. 160 (1985) 122.
[9] V.A. Burrows, S. Sundaresan, Y.J. Chabal, S.B. Christman, Surf. Sci. 180 (1987) 110.
[10] G. Ertl, Science 254 (1991) 1750.
[11] H.H. Rotermund, W. Engel, M. Kordesch, G. Ertl, Nature 343 (1990) 355.
[12] M. Bron, D. Teschner, A. Knop-Gericke, B. Steinhauer, A. Scheybal, M. Hävecker, D. Wang, R. Födisch, D. Hönicke, A. Wootsch, R. Schlögl, P. Claus, J. Catal. 234 (2005) 37.
[13] T. Ressler, M. Hagelstein, U. Hatje, W. Metz, J. Phys. Chem. B 101 (1997) 6680.
[14] S.J.A. Figueroa, M.A. Newton, J. Catal. 312 (2014) 69.
[15] M. Newton, Catalysts 7 (2017) 58.
[16] B.C. Sales, J.E. Turner, M.B. Maple, Surf. Sci. 114 (1982) 381.
[17] J.E. Turner, M.B. Maple, Surf. Sci. 147 (1984) 647.
[18] N. Hartmann, R. Imbihl, W. Vogel, Catal. Lett. 28 (1994) 373.
[19] A.B. Kroner, M.A. Newton, M. Tromp, A.E. Russell, A.J. Dent, J. Evans, Catal. Struct. React. 3 (2017) 13.
[20] M.A. Newton, A.J. Dent, J. Evans, Chem. Soc. Rev. 31 (2002) 83.
[21] O. Müller, M. Nachtegaal, J. Just, D. Lützenkirchen-Hecht, R. Frahm, J. Synchro. Radiat. 23 (2016) 260.
[22] S. Diaz-Moreno, M. Amboage, M. Basham, R. Boada, N.E. Bricknell, G. Cibin, T. M. Cobb, J. Filik, A. Freeman, K. Geraki, D. Gianolio, S. Hayama, K. Ignatyev, L. Keenan, I. Mikulska, J.F.W. Mosselmans, J.J. Mudd, S.A. Parry, J. Synchro. Radiat. 25 (2018) 998.
[23] P.-A. Carlsson, L. Österlund, P. Thormählen, A. Palmqvist, E. Fridell, J. Jansson, M. Skoglundh, J. Catal. 226 (2004) 422.
[24] J. Singh, M. Nachtegaal, E.M.C. Alayon, J. Stötzel, J.A. van Bokhoven, ChemCatChem 2 (2010) 653.
[25] J. Singh, J.A. van Bokhoven, Catal. Today 155 (2010) 199.
[26] M.A. Newton, D. Ferri, G. Smolentsev, V. Marchionni, M. Nachtegaal, Nat. Commun. 6 (2015) 8675.
[27] J. Singh, M. Tromp, O.V. Safonova, P. Glatzel, J.A. van Bokhoven, Catal. Today 145 (2009) 300.
[28] J. Singh, E.M.C. Alayon, M. Tromp, O.V. Safonova, P. Glatzel, M. Nachtegaal, R. Frahm, J.A. van Bokhoven, Angew. Chem. Int. Ed. 47 (2008) 9260.
[29] M.A. Newton, W. van Beek, Chem. Soc. Rev. 39 (2010) 4845.
[30] E.K. Dann, E.K. Gibson, R.A. Catlow, P. Collier, T. Eralp Erden, D. Gianolio, C. Hardacre, A. Kroner, A. Raj, A. Goguet, P.P. Wells, Chem. Mater. 29 (2017) 7515.
[31] M.A. Newton, A.J. Dent, S. Diaz-Moreno, S.G. Fiddy, B. Jyoti, J. Evans, Chem. – Euro. J. 12 (2006) 1975.
[32] A.M. Gänzler, M. Casapu, A. Boubnov, O. Müller, S. Conrad, H. Lichtenberg, R. Frahm, J.-D. Grunwaldt, J. Catal. 328 (2015) 216.
[33] C. Stewart, E.K. Gibson, K. Morgan, G. Cibin, A.J. Dent, C. Hardacre, E.V. Kondratenko, V.A. Kondratenko, C. McManus, S. Rogers, C.E. Stere, S. Chansai, Y.-C. Wang, S.J. Haigh, P.P. Wells, A. Goguet, ACS Catal. (2018) 8255.
[34] A. Goguet, C. Stewart, J. Touitou and K. Morgan, in A.G. Dixon and O. Deutschmann (Editors), Advances in Chemical Engineering, Vol. 50, Academic Press, p. 131; 2017.
[35] M.A. Newton, J.B. Brazier, E.M. Barreiro, S. Parry, H. Emmerich, L.A. Adrio, C.J. Mulligan, K. Hellgardt, K.K. Hii, Green Chem. 18 (2016) 406.
[36] J.D. Grunwaldt, M. Caravati, S. Hannemann, A. Baiker, PCCP 6 (2004) 3037.
[37] J.-C. Labiche, O. Mathon, S. Pascarelli, M.A. Newton, G.G. Ferre, C. Curfs, G. Vaughan, A. Homs, D.F. Carreiras, Rev. Sci. Instrum. 78 (2007) 091301.
[38] D.C. Koningsberger, B.L. Mojet, G.E. van Dorssen, D.E. Ramaker, Top. Catal. 10 (2000) 143.
[39] A.M. Beale, B.M. Weckhuysen, PCCP 12 (2010) 5562.
[40] S.C. Su, J.N. Carstens, A.T. Bell, J. Catal. 176 (1998) 125.
[41] S.M. Rogers, C.R.A. Catlow, C.E. Chan-Thaw, A. Chutia, N. Jian, R.E. Palmer, M. Perdjon, A. Thetford, N. Dimitratos, A. Villa, P.P. Wells, ACS Catal. 7 (2017) 2266.
[42] X. Wang, H. Shi, J.H. Kwak, J. Szanyi, ACS Catal. 5 (2015) 6337.
[43] R.P. Eischens, S.A. Francis, W.A. Pliskin, J. Phys. Chem. 60 (1956) 194.
[44] D. Tessier, A. Rakai, F. Bozon-Verduraz, J. Chem. Soc. Faraday Trans. 88 (1992) 741.
[45] G.C. Cabilla, A.L. Bonivardi, M.A. Baltanás, Catal. Lett. 55 (1998) 147.
[46] A.M. Bradshaw, F. Hoffmann, Surf. Sci. 52 (1975) 449.
[47] N.D. Parkyns, J. Phys. Chem. 75 (1971) 526.
[48] J. Szanyi, J.H. Kwak, PCCP 16 (2014) 15126.
[49] A.M. Bradshaw, F.M. Hoffmann, Surf. Sci. 72 (1978) 513.
[50] M. Bowker, Chem. Soc. Rev. 37 (2008) 2204.
[51] C.T. Campbell, G. Ertl, H. Kuipers, J. Segner, J. Chem. Phys. 73 (1980) 5862.
[52] T. Engel, G. Ertl, J. Chem. Phys. 69 (1978) 1267.